

## Influence of small polarons on the optical properties of Mg:LiNbO<sub>3</sub> crystals

G. Kh. Kitaeva, K. A. Kuznetsov, and A. N. Penin

*Department of Physics, Moscow State University, 119899 Moscow, Russia*

A. V. Shepelev

*A. N. Kosygin Moscow State Textile University, 117918 Moscow, Russia*

(Received 8 June 2001; published 14 January 2002)

We have measured refractive indices and absorption coefficients for Mg:LiNbO<sub>3</sub> single crystals of different Mg contents (0–7 mol%) in the visible and IR ranges up to the phonon absorption edge. The obtained dependencies of optical characteristics on Mg concentration in an IR region of 4–5 μm indicate the four-step character of structural changes under subsequent Mg doping. Spectral dependencies of optical characteristics reveal the existence of two polaron resonance bands, centered at 1.3 and 3.2 μm, which are not observed in the pure LiNbO<sub>3</sub>. The theory approximation of the band at 1.3 μm, enhanced after chemical reduction, enabled us to determine the main polaron parameters for the 1.3-μm band, and to make a possible assignment of the 3.2 μm band. We assign this to direct transitions between energy levels of polarons trapped at Nb<sub>Nb</sub> sites and those of polarons trapped at Nb<sub>Li</sub> antisites in a lattice. A number of peculiarities are revealed in the absorption behavior at the low-energy edge from 1000 to 3000 cm<sup>-1</sup>. The values of the uninduced part of absorption are sufficiently less than those predicted by a phonon oscillator model. Absorption spectral dependencies are modulated at a rather stable period, being of the order of frequencies of the lowest-energy longitudinal optical phonons, excited at a room temperature.

DOI: 10.1103/PhysRevB.65.054304

PACS number(s): 71.38.Ht, 78.20.Ci

Bulk crystals of doped LiNbO<sub>3</sub> are important for a variety of applications using nonlinear optical,<sup>1</sup> ferroelectric,<sup>2</sup> and photorefractive<sup>3</sup> effects. Different doping atoms enter into the defect structure of nonstoichiometric crystals and change it in different ways. As a result, some dopants (like Fe or Cu) are used to increase the photorefractive sensitivity to light. The others (Mg, Sc, Zn) are necessary to improve the resistance to optical damage in nonlinear optical devices.<sup>4</sup> At the same time, the incorporation of doping agents, or the changing of the nonstoichiometric composition, essentially modify the optical characteristics of LiNbO<sub>3</sub> crystals in its transparency region.<sup>5,6</sup>

Accurate data on refractive indices are required for a variety of applications. Refractive indices were measured for concrete type of LiNbO<sub>3</sub> crystal: for undoped LiNbO<sub>3</sub> crystals of different nonstoichiometric composition,<sup>7–11</sup> for differently Mg-doped crystals,<sup>12–18</sup> and others. Zelmon, Small, and Jundt<sup>16</sup> obtained Sellmeier equations for the largest spectral interval for congruent LiNbO<sub>3</sub> and for Mg:LiNbO<sub>3</sub>, grown from the melt of 5 mol% MgO. Their equations fit refractive indices dispersions in the total region 0.4–5 μm with the best overall absolute accuracy within ±0.0002.

Betzler and Schlarb<sup>14,15</sup> proposed a more general approach. They tried to predict the dependence of the refractive index dispersion law on the crystal composition. They obtained generalized Sellmeier equations for the wavelength range from 400 to 1200 nm with an account for the defect structure of Li-deficient LiNbO<sub>3</sub> crystals.<sup>14</sup> Later,<sup>15</sup> they deduced the generalized Sellmeier equations for all Mg-doped Li-deficient crystals. To obtain the best fit to experimental results in the visible and in the near-IR range, changes of electronic oscillator terms under variation of crystal composition were considered.

In previous works,<sup>11,12,17</sup> we measured the ordinary refractive index dispersion for different types of LiNbO<sub>3</sub> crystals in the middle IR region by spontaneous parametric light scattering method. Here we analyze our last results<sup>18</sup> on the ordinary refractive index dispersion in differently doped Mg:LiNbO<sub>3</sub>, measured in visible and infrared ranges up to 5 μm. The main result of our treatment consists of the following: it is impossible to construct a microscopic model of dispersion without taking into account a possible formation of polarons in lithium niobate crystals. We studied the absorption dispersion of reduced and unreduced crystals, before and after light illumination. We conclude that to account for polaron resonances is important even for crystals, which were not exposed to chemical reduction.

The study of optical properties of doped LiNbO<sub>3</sub> crystals enables one to solve more general problems concerning the nature of small polaron mobility and its influence on the optical response function of crystals.<sup>19</sup> This problem is extensively studied starting with the earlier works in the 1950s,<sup>20</sup> and up to the present. Many experimentally observed characteristics of polaronic absorption remain unexplained, mainly in the low-energy parts of spectra. On the other hand, several theoretically predicted effects, such as transitions without phonon assistance, interband transitions, were studied purely experimentally. Properties of bound polarons, such as bipolarons, are of special interest.

Polaron resonances in the pure LiNbO<sub>3</sub> crystals were studied rather explicitly.<sup>21–28</sup> Sufficiently less information is available on polarons in the doped LiNbO<sub>3</sub>.<sup>26,29,30</sup> We report on absorption resonances observed by the Fourier spectroscopy method in Mg:LiNbO<sub>3</sub>. The dispersion of the absorption coefficient in the region of these resonances has a distinctive spectral behavior with phonon iterations. To understand the origin of the resonances we studied the

TABLE I. Parameters of bulk Mg:LiNbO<sub>3</sub> crystals

No.	Molar concentration of Mg(%)	Reduction conditions	The angle of second-harmonic generation 1.06 $\mu\text{m}$ $\rightarrow$ 0.532 $\mu\text{m}$ , degrees
1	0	-	
2	4.4 $\pm$ 0.1	-	75.9
2.1	4.4 $\pm$ 0.1	at 500 $^{\circ}\text{C}$ , $P = 10^{-5}$ Torr	
3	5.1 $\pm$ 0.1	-	77.5
4	5.7 $\pm$ 0.4	-	82.1
5	6.1 $\pm$ 0.2	-	82.8
6	7.1 $\pm$ 0.2	-	85.8
6.1	7.1 $\pm$ 0.2	at 600 $^{\circ}\text{C}$ , $P = 10^{-5}$ Torr	

changes in absorption spectra after chemical reduction or illumination by intense visible and IR laser sources.

Section I of this paper contains characteristics of used samples. Experimental results on spectral and concentration dependencies of refractive indices and absorption coefficients are presented in Secs. II and III. More general conclusions, following from the concrete behavior of measured characteristics, are discussed in Sec. IV. They are mainly related to the polaronic nature of resonance bands in the spectral region, where common pure LiNbO<sub>3</sub> is usually treated as transparent. The most notable part of them is formulated in Sec. V.

## I. CHARACTERISTICS OF THE CRYSTALS

We used bulk Mg:LiNbO<sub>3</sub> single crystals, grown by the Czochralski method. The starting material was close to congruently melting composition with the ratio Li/Nb=0.942.<sup>31</sup> The MgO doping concentration varied from 0 to about 7 mol % under growth of different samples. The final concentration and spatial distribution of Mg in the grown crystals was studied by means of the fluorescent x-ray spectral analysis and wave dispersive x-ray microanalysis. The spatial variation of Mg-concentration in the samples was within  $\pm 0.01$ –0.03 mol %. The measurements of distribution of the impurity concentration within each crystal were made by x-ray microanalysis using Camebax SX-50 with a high relative accuracy. However, an absolute error of the value of an average Mg concentration was sufficiently larger, and exceeded 0.4 mol % for one of the crystals (see Table I).

Concerning the variation of LiNbO<sub>3</sub> defect structure under Mg doping, most models<sup>4,22,26,29,32–34</sup> agree that there is a threshold in Mg concentration, above which the crystal structure and properties change qualitatively. Above this threshold concentration  $C_{\text{thr}}$ , all defect atoms of Nb in Li antisites ( $\text{Nb}_{\text{Li}}$ ) are replaced by Mg.<sup>32</sup> The crystal becomes optically resistant and loses most of its photorefractivity.<sup>33</sup> For a congruent Li/Nb composition, threshold concentration  $C_{\text{thr}} \sim 5$  mol %. Thus the Mg concentration of the most of crystals in Table I is above  $C_{\text{thr}}$ . For one of the crystals  $C_{\text{Mg}} = 4.4$  mol %  $< C_{\text{thr}}$ , and one is nominally pure:  $C_{\text{Mg}} = 0$ .

Two grown crystals, of  $C_{\text{Mg}} = 4.4$  mol %  $< C_{\text{thr}}$  and of  $C_{\text{Mg}} = 7.1$  mol %  $> C_{\text{thr}}$ , were cut in two parts. One part of

each crystal was chemically reduced in a vacuum ( $P = 10^{-5}$  Torr). The reduction temperature was 500  $^{\circ}\text{C}$  in the case of  $C_{\text{Mg}} < C_{\text{thr}}$  and 600  $^{\circ}\text{C}$  in the case of  $C_{\text{Mg}} > C_{\text{thr}}$ .

Triangular prisms were cut for refractive index measurements in the visible range. The input and output polished surfaces of each prism were oriented along the crystal  $C$  axis, with an angle of  $\sim 30^{\circ}$  between them. For measurements of absorption and refractive indices in the IR range, the samples were cut in the form of rectangular parallelepipeds. Input and output polished surfaces were also oriented along  $C$  axis. Absorption measurements were carried out in the samples of different thicknesses. The sample of the smallest thickness 8  $\mu\text{m}$  was prepared by polishing of the undoped LiNbO<sub>3</sub>. It was enclosed between two polished plates of the crystal BaF<sub>2</sub>.

## II. REFRACTIVE INDEX DISPERSION

We have measured the dispersion characteristics of ordinary ( $n_o$ ) and extraordinary ( $n_e$ ) refractive indices of the crystals in the visible range at room temperature by the prism method, using a goniospectrometer. The absolute error did not exceed  $\pm 0.0002$ . Refractive indices at 1.06  $\mu\text{m}$  were measured with the help of an image-converting visualiser. The obtained data in the region 0.4–1.06  $\mu\text{m}$  were fitted by Sellmeier-type equations with coefficients differing for the differently doped samples.<sup>18</sup> In this form they were used in subsequent measurements of the ordinary refractive indices in the IR range, made by two nonlinear-optical methods (Table II).

In the region of 1–1.25  $\mu\text{m}$  the values of  $n_o$  were determined by measuring of the angle for second harmonic generation of a yttrium aluminum garnet (YAG):Nd laser and of a tunable LiF:F<sub>2</sub> laser. To calculate the  $n_o(\lambda)$  values, the results for  $n_e(\lambda/2)$  in the visible region were taken into account. We estimate the total absolute error of the obtained data as  $\pm 0.0005$ .

In the region of 2–5  $\mu\text{m}$  the values of  $n_o(\lambda)$  were obtained by spontaneous parametric light scattering (the down-conversion) method. The optical scheme<sup>18</sup> included an Ar laser as a pump source at 0.488 nm. The pump wave was polarized extraordinarily, and the visible signal and IR idle waves were polarized ordinarily. The position of maximum

TABLE II. Refractive indices  $n_o$  in the IR range.

Wavelength (nm)	Molar concentration of Mg(%)					
	0	4.4±0.1	5.1±0.1	5.7±0.4	6.1±0.2	7.1±0.2
1.064		2.2281	2.2277	2.2250	2.2231	2.2222
1.1334	2.229	2.2244	2.2238	2.2216	2.2193	2.2183
1.246	2.2206					
2.124	2.1937	2.1910	2.1841	2.1805	2.1798	2.1810
2.241	2.1869	2.1831	2.1807	2.1769	2.1752	2.1769
2.348	2.1825	2.1827	2.1772	2.1732	2.1713	2.1737
2.596	2.1710	2.1731	2.1659	2.1619	2.1625	2.1627
2.802	2.1593	2.1643	2.1582	2.1545	2.1525	2.1534
3.050	2.1471	2.1482	2.1482	2.1423	2.1413	2.1409
3.359	2.1341	2.1335	2.1336	2.1265	2.1244	2.1269
3.759	2.1097	2.1158	2.1127	2.1061	2.1013	2.1053
4.296	2.069	2.074	2.078	2.070	2.065	2.069
4.927	2.018	2.018	2.033	2.018	2.010	2.015

for the angle distribution of a visible signal intensity was measured for each IR idle wavelength. At these angles, exact phase matching conditions  $\mathbf{k}_p = \mathbf{k}_s + \mathbf{k}_i$  connect the wave vectors of the pump ( $\mathbf{k}_p$ ), signal ( $\mathbf{k}_s$ ), and idle ( $\mathbf{k}_i$ ) waves in a crystal. It enables to determine the wave vectors  $k_i = n_i \omega_i / c$  and refractive indices  $n_i$  of idle waves in a crystal transparency region, if the values of the wave vectors of signal and pump waves are known. The data on refractive indices in the visible range were used to determine  $k_p$  and  $k_s$ . The absolute error of  $n_o$  values, obtained by this method, grows with the wavelength, being near  $\pm 0.0005$  at  $2 \mu\text{m}$  and exceeding  $\pm 0.002$  at  $5 \mu\text{m}$ . An exact treatment<sup>35</sup> showed, that in the absorption region, this method gives a value of  $n_{\text{eff}} \equiv \sqrt{\epsilon'}$ , where  $\epsilon'$  is the real part of a complex dielectric constant  $\epsilon = \epsilon' + i\epsilon''$  at the idle wavelength.  $n_{\text{eff}}$  coincides with the value of the refractive index  $n$  if  $\epsilon''$  is negligible.

An attractive result follows from a comparison of refractive indices of crystals of different Mg concentrations, taken at constant wavelengths. In Fig. 1 the concentration dependencies of deviations  $\Delta\epsilon'_o(C_{\text{Mg}}, \lambda) \equiv \epsilon'_o(C_{\text{Mg}}, \lambda) - \epsilon'_o(0, \lambda) = n_o^2(C_{\text{Mg}}, \lambda) - n_o^2(0, \lambda)$  are presented for several fixed wavelengths in the visible and IR ranges.  $\Delta\epsilon'_o(C_{\text{Mg}})$  describes the deviation of the real part for the ordinary dielectric constant of a doped crystal from that of an undoped  $\text{LiNbO}_3$ . All crystals were grown from a melt of the same Li/Nb ratio. In the visible and near-infrared regions each  $\Delta\epsilon'_o(C_{\text{Mg}})$  experimental dependence looks like a piecewise-linear function with a single break near  $C_{\text{thr}}$ . Betzler and Shlarb<sup>15</sup> put just the same dependence into the basis of their generalized Sellmeier equations in the region  $0.4\text{--}1.2 \mu\text{m}$ . But when the wavelength increases and approaches the phonon absorption edge, the more complex character of  $\Delta\epsilon'_o(C_{\text{Mg}})$  becomes apparent in our results.

To explain this, consider how the values of a dielectric constant change under crystal structure variation. Values of a dielectric constant at given wavelengths are dependent on

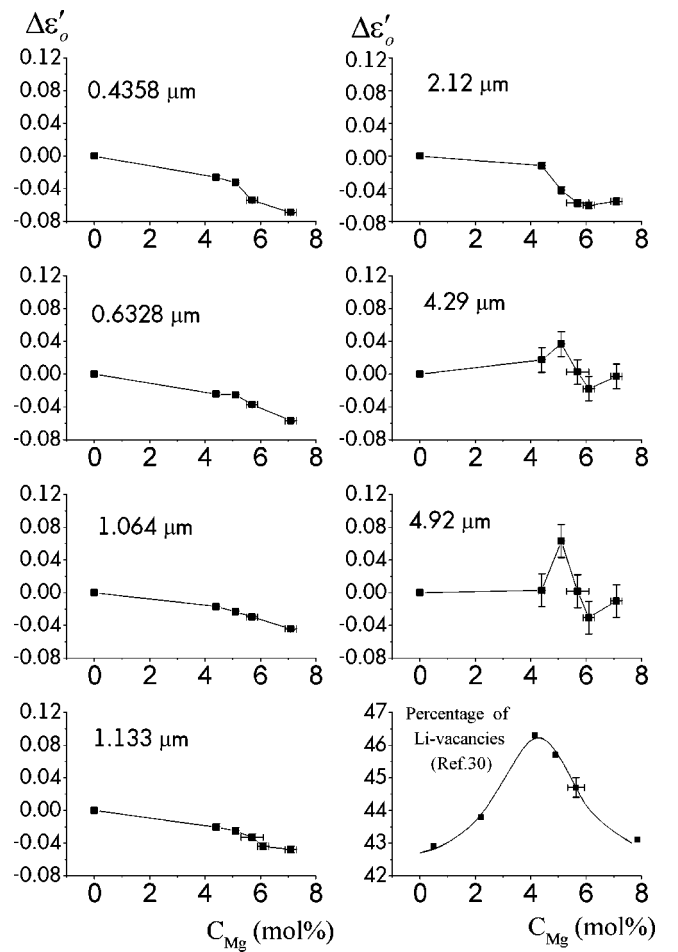


FIG. 1. Measured dependencies of  $\Delta\epsilon'_o(C_{\text{Mg}}, \lambda)$  as a function of Mg concentration  $C_{\text{Mg}}$  in  $\text{Mg}:\text{LiNbO}_3$  crystals for different wavelengths  $\lambda$  in the visible and IR spectral regions. The last plot (data from the Ref. 32) shows the molar concentration of  $\text{Li}^+$  vacancies on regular cation sites as a function of the Mg concentration.

oscillator strengths of resonance terms, which describe the separate contributions of core vibrations and electronic transitions into the optical response. In turn, oscillator strengths are proportional to the corresponding ion concentrations and change under doping ion incorporation into the crystal structure. The two-step piecewise-linear behavior of  $\Delta\epsilon'_o(C_{\text{Mg}})$  is a consequence of the simplest two-step model of Mg incorporation into  $\text{LiNbO}_3$  crystal. According to this model, at low  $C_{\text{Mg}}$ , when  $C_{\text{Mg}} < C_{\text{thr}}$ , Mg substitutes gradually for antisite Nb ions, i.e.,  $\text{Mg}_{\text{Li}} \rightarrow \text{Nb}_{\text{Li}}$ . At  $C_{\text{Mg}} = C_{\text{thr}}$  all  $\text{Nb}_{\text{Li}}$  defects are replaced, and this process stops. At the same time, other substitution processes (like  $\text{Mg}_{\text{Li}} \rightarrow \text{Li}_{\text{Li}}$ , for example) expand continuously under  $C_{\text{Mg}}$  growth and also remain at  $C_{\text{Mg}} > C_{\text{thr}}$ . The dielectric constant dependence on  $C_{\text{Mg}}$  near the UV absorption edge is most sensitive to electronic oscillator terms. Conversely, near the phonon absorption edge, the behavior of vibration resonance terms just determines the dielectric constant dependence. Our results show that vibration resonance terms are more sensitive to structure variations in case of  $\text{Mg}:\text{LiNbO}_3$ . When the wavelength approaches the phonon absorption edge, it appears that the real model of Mg incorporation is much more complex, than it follows from the  $n_o(C_{\text{Mg}})$  in the short-wavelength range up to  $1 \mu\text{m}$ . As seen in Fig. 1, at  $\lambda = 4\text{--}5 \mu\text{m}$ , up to four character steps in the Mg incorporation mechanism can exist in the region of  $C_{\text{Mg}} = 0\text{--}7 \text{ mol } \%$ . This result was predicted by Donnerberg *et al.* in their computer simulation studies of Mg incorporation mechanism.<sup>32</sup> Also, it is interesting to note that the character of our experimental  $\Delta\epsilon'_o(C_{\text{Mg}})$  dependencies in the IR region is similar to the character of  $C_{\text{Mg}}$  dependence of Li vacancies on regular cation sites<sup>32</sup> (last plot in Fig. 1).

We made attempts to fit spectral dependencies obtained for the IR region by equations of the Sellmeier type. But all such formulas were too rough, and did not coincide with the measured values within any appropriate accuracy. Indeed, the Sellmeier equation accounts for the total contribution of different oscillator terms in the region far from the resonance frequencies. It can be used for spectral regions where dispersion has a continuous monotonic character, without any oscillator behavior. In our case, the precise shapes of dispersion curves were not monotonic in the spectral region usually accepted as a transparency region for  $\text{Mg}:\text{LiNbO}_3$  crystals. It is easily seen in the spectral dependencies of the deviations  $\Delta\epsilon'_o(C_{\text{Mg}}, \lambda)$ , presented in Fig. 2 for the doped crystals of different  $C_{\text{Mg}}$ . Far from phonon and electronic resonance frequencies, each dielectric constant  $\epsilon'_o(C_{\text{Mg}}, \lambda)$  and  $\epsilon'_o(0, \lambda)$  should decrease monotonically when the wavelength increases. As a consequence, the deviation  $\Delta\epsilon'_o(C_{\text{Mg}}, \lambda)$  in the region of  $0.4\text{--}5 \mu\text{m}$  should also increase or decrease monotonically. The experiment shows that it is not so, thus, there are additional intrinsic resonances in the studied region.

The broad resonances centered at  $0.5$  and  $0.75 \mu\text{m}$  are well-known for pure congruent  $\text{LiNbO}_3$ . They are observed in absorption spectra of reduced crystals and are attributed to small polaron and bipolaron transitions.<sup>22,23,25</sup> An electron trapped at  $\text{Nb}_{\text{Li}}$  forms a small polaron, two electrons trapped at neighboring  $\text{Nb}_{\text{Li}}$  and  $\text{Nb}_{\text{Nb}}$  form a bipolaron in  $\text{LiNbO}_3$ . The IR resonance centered near  $1.3 \mu\text{m}$  was observed in

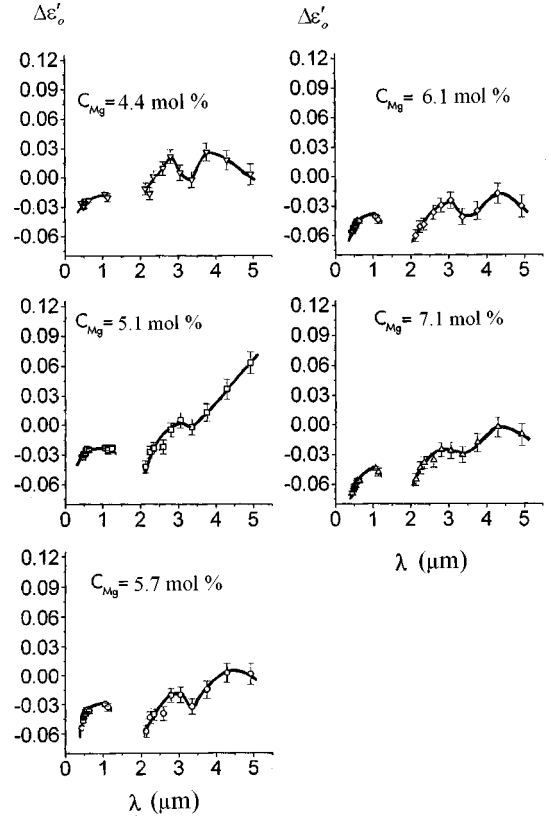


FIG. 2. Dispersion of the deviation  $\Delta\epsilon'_o(C_{\text{Mg}}, \lambda) \equiv \epsilon'_o(C_{\text{Mg}}, \lambda) - \epsilon'_o(0, \lambda)$  of the dielectric constant of the doped  $\text{Mg}:\text{LiNbO}_3$  [ $\epsilon'_o(C_{\text{Mg}}, \lambda)$ ] from the dielectric constant of a pure  $\text{LiNbO}_3$  [ $\epsilon'_o(0, \lambda)$ ] for different concentrations of Mg dopant.

absorption spectra for reduced  $\text{Mg}:\text{LiNbO}_3$ ,<sup>34</sup> and later it was attributed to the small polarons self-trapped at regular  $\text{Nb}_{\text{Nb}}$ .<sup>26</sup> The same resonances were found and used for holograms IR readouts and recording in other doped  $\text{LiNbO}_3$ .<sup>3,30</sup> Virtually, the band parameters are independent on the dopant ion type.<sup>26</sup> The resonance near  $1.3 \mu\text{m}$  also appears in our dispersion curves  $\Delta\epsilon'_o(\lambda)$  for unreduced crystals. It can be seen in Fig. 2, that the resonance behavior of the real part of a dielectric constant in this region becomes more pronounced after a threshold Mg concentration at 5 mol %. In addition, there are additional resonances in the region of  $2\text{--}5 \mu\text{m}$ . The most pronounced resonance behavior at  $2.8\text{--}3.5 \mu\text{m}$  is outside the error limits.

The observed nonmonotonic behavior of a dielectric constant dispersion could be due to polaronic (or some other) defects in unreduced crystals. To understand the origin of the observed dielectric constant dispersion, we examined the absorption spectra of  $\text{Mg}:\text{LiNbO}_3$  before and after a chemical reduction.

### III. IR ABSORPTION OF REDUCED AND UNREDUCED CRYSTALS

We have measured transparency in the visible and IR ranges for the samples of different thickness at room temperature. The thickness of bulk samples was in the range

0.5–12 mm, and the thickness of a thin film was 8  $\mu\text{m}$ . Measurements in the spectral interval of 2–8  $\mu\text{m}$  were made by means of Fourier-spectroscopy, with a spectral resolution of 1.5  $\text{cm}^{-1}$ .

Calculations of absorption coefficients were made neglecting anisotropy effects. To determine absorption coefficients  $\alpha$ , as a rule, we eliminated the reflection losses, accounting for the measured values of ordinary refractive index. Since the refractive index values were determined in the range up to 5  $\mu\text{m}$  only, and in quite rare spectral points, we extrapolated the known values to the unmeasured spectral intervals. Obviously, such smoothed curves for refractive index dispersion were deprived of the fine peculiarities, which were seen on transparency curves, remaining on dispersion curves for  $\alpha$ . To decrease the probable errors caused by this factor, we determined absorption coefficients over a relation between transmission data for the samples of different thickness, cut from the same crystal material. Obtained in this way, results on  $\alpha$  coincided very well in most of details with the results obtained by the first approach for the samples of near 1-cm thickness. Thus the corresponding details in refractive index dispersion, or other possible surface effects, are not so significant for samples of 1 cm and more. But there was not numerical coincidence between the results for  $\alpha$  in a thin film of 8- $\mu\text{m}$  thickness, and in bulk  $\text{LiNbO}_3$  samples of several millimeters. Indeed, in this case our extracting of reflection losses seems to be too rough, since the relative contribution of surface effects is much more higher for a 8- $\mu\text{m}$  film. There can be different kinds of surface effects. First of all, the presence of modulation in final absorption curves indicates that some kind of modulation exists in refractive index dispersion also, but we do not account it in our calculations of reflection losses. Next the structure of crystal defects,<sup>22</sup> and the corresponding values of optical characteristics at a surface are not the same as in the crystal volume. Possible interference effects were not taken into account also. Nevertheless, we still present below the results obtained for this thin film, since they indicate qualitatively the absorption dispersion character at the lowest available photon energies.

Figure 3 presents results obtained in the whole measured range at room temperatures for the reduced  $\text{Mg}:\text{LiNbO}_3$ ; for comparison, absorption coefficient dispersion for one of the unreduced crystals is shown also. Although the crystal with the Mg concentration before threshold value  $C_{\text{Mg}} = 4.4 \text{ mol \%} < C_{\text{thr}}$  was reduced at smaller temperature, its absorption was sufficiently larger. We cite the most confident part of the whole curve for this crystal, the amplitude of the observed noise becomes too large at higher photon energies. As expected, dispersion of  $\alpha$  in the range up to 5  $\mu\text{m}$  in a crystal with the highest  $C_{\text{Mg}} = 7.1 \text{ mol \%} > C_{\text{thr}}$  is characterized by a single broad peak centered at 1.3  $\mu\text{m}$  (the corresponding photon energy is 0.94 eV). At  $\lambda > 4 \mu\text{m}$  an additional structure appears, it will be discussed below. Absorption of another reduced crystal of  $C_{\text{Mg}} = 4.4 \text{ mol \%} < C_{\text{thr}}$  has an additional peak at 3.2  $\mu\text{m}$  (0.38 eV). The position of the peak agrees with the spectral region of anomalous dispersion of  $\Delta\epsilon'_0(\lambda)$ , obtained for all Mg-doped unreduced crystals (compare Figs. 2 and 3).

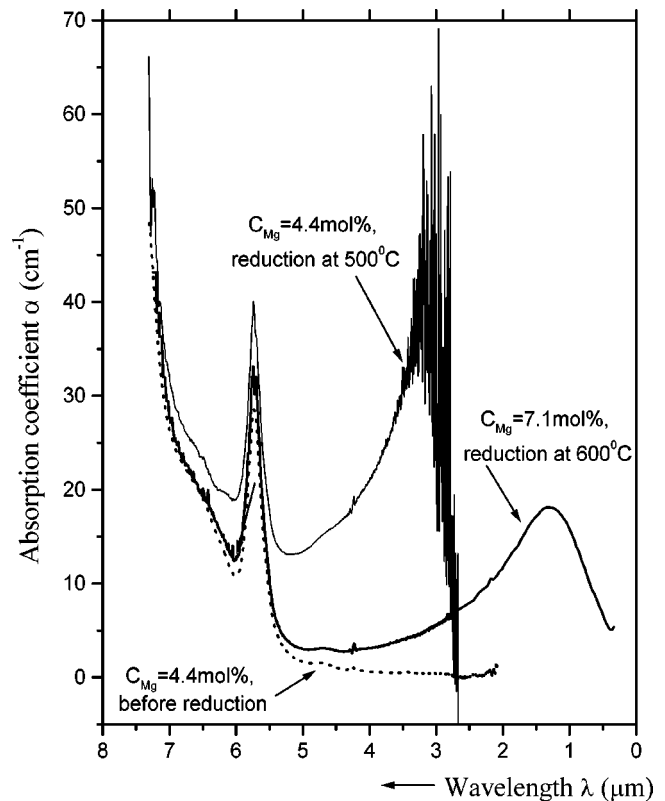


FIG. 3. Influence of Mg concentration on absorption spectra of reduced  $\text{Mg}:\text{LiNbO}_3$  crystals. Solid curves:  $\alpha$  for samples 6.1 and 2.1; dotted curve:  $\alpha$  for the sample 6 before reduction.

The residual small absorption was observed in the region of this peak in unreduced crystals, doped by Mg (Figs. 4 and 5). For one of the unreduced crystals ( $C_{\text{Mg}} = 7.1 \text{ mol \%}$ ), absorption was measured after exposition to power laser radiation at 1.06 and 0.532  $\mu\text{m}$  during several hours. The power density was near  $10^6 - 10^7 \text{ W/cm}^2$ , and the total energy radiation dose was  $10^3 - 10^4 \text{ J/cm}^2$ . Figure 4 presents absorption dispersion on a logarithmic scale, obtained for reduced and unreduced crystals. The value of additional absorption, induced by laser radiation, is much smaller, but its spectral behavior looks similar to the spectral dependence of absorption changes due to reduction in the crystal of  $C_{\text{Mg}} = 4.4 \text{ mol \%}$ . The spectra of unilluminated unreduced Mg-doped crystals replicate each other, and distinct from the spectra of the unreduced nominally pure  $\text{LiNbO}_3$  crystal in the spectral region of the 3.2- $\mu\text{m}$  peak ( $2.500 - 3.500 \text{ cm}^{-1}$ ). It is necessary to note that residual light-induced absorption changes were not observed in a pure  $\text{LiNbO}_3$  crystal.

The influence of effects induced by reduction or illumination decreases at the lowest achieved frequencies. After subtraction of all induced effects, the crystals seem to exhibit quite the same absorption coefficient in the region below  $2500 \text{ cm}^{-1}$ . Only the crystal of a threshold concentration  $C_{\text{Mg}} = 5.1 \text{ mol \%}$  has a slightly higher values of  $\alpha$ . It is seen in the range of 4–5  $\mu\text{m}$ . The character of absorption dependence on concentration  $C_{\text{Mg}}$  replicates the dependence of  $\Delta\epsilon'_0(C_{\text{Mg}})$  at 4–5  $\mu\text{m}$ , shown in Fig. 1.

The special attention should be paid to the low-frequency

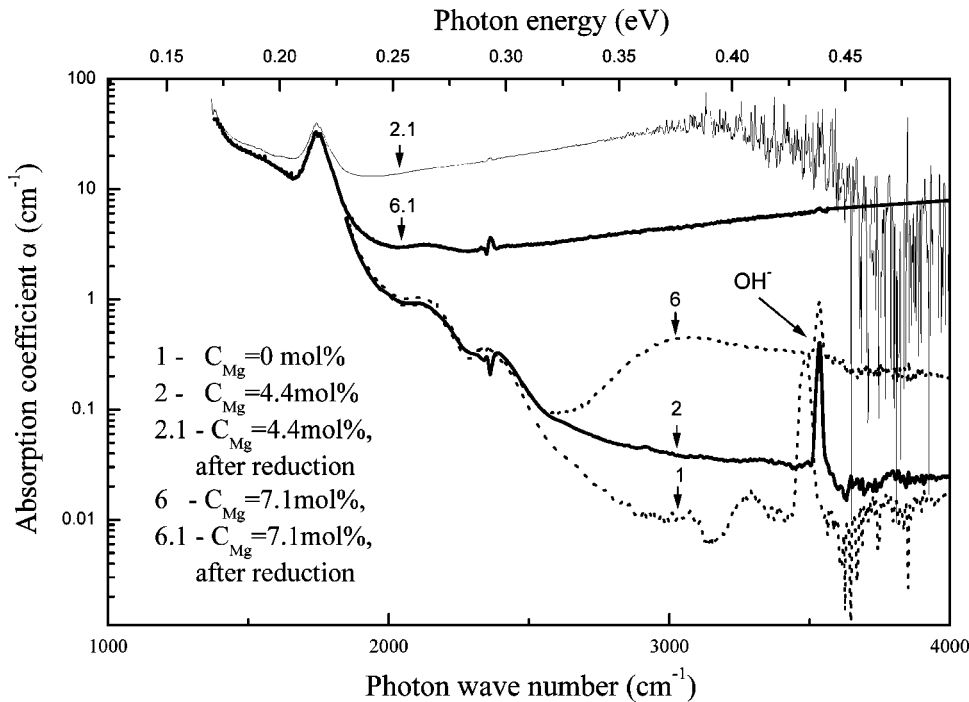


FIG. 4. Absorption at phonon edge of transparency region for Mg:LiNbO<sub>3</sub> crystals of different Mg contents, before and after chemical reduction.

modulation of spectra in that regions, where induced effects are weak. The period of modulation is near 200 cm<sup>-1</sup>. The modulation has a well-pronounced character in a region from 1500 up to 2500 cm<sup>-1</sup>. When the induced absorption is present, it looks like a continuous background added to a modulated part. The modulated part itself seems to be independent of reduction or light illumination. One of the peaks is much greater than the others—it looks like a sharp absorption line at 1740 cm<sup>-1</sup> (5.75 μm, 0.2 eV). Such a modulation exists in absorption spectra of all doped Mg:LiNbO<sub>3</sub> and undoped LiNbO<sub>3</sub> crystals.

#### IV. DISCUSSION

The whole disposal of absorption changes seems to be quite complicated. To simplify the analysis, let us eliminate two different contributions into each absorption curve  $\alpha(\omega)$ :

$$\alpha(\omega) = \alpha_{\text{ind}}(\omega) + \alpha_0(\omega). \quad (1)$$

$\alpha_{\text{ind}}(\omega)$  is a part of the absorption, induced by chemical reduction or laser irradiation;  $\alpha_0(\omega)$  is a residual part of the absorption, which is originally peculiar to each crystal.

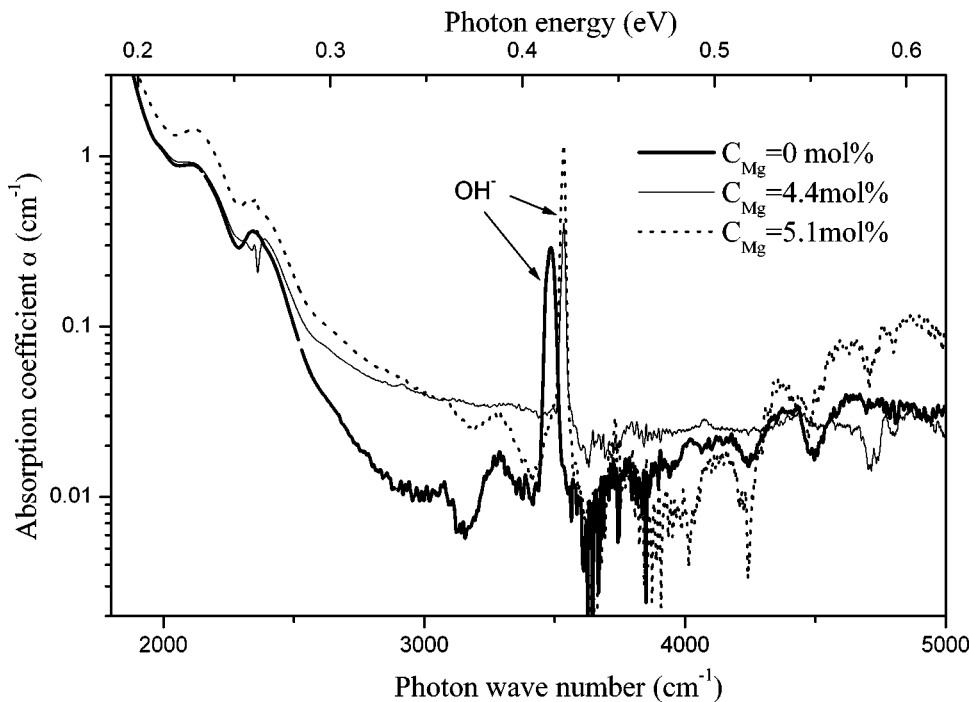


FIG. 5. Fragments of absorption spectra of Mg:LiNbO<sub>3</sub> crystals before chemical reduction: a low-frequency modulation at small  $\alpha$ .

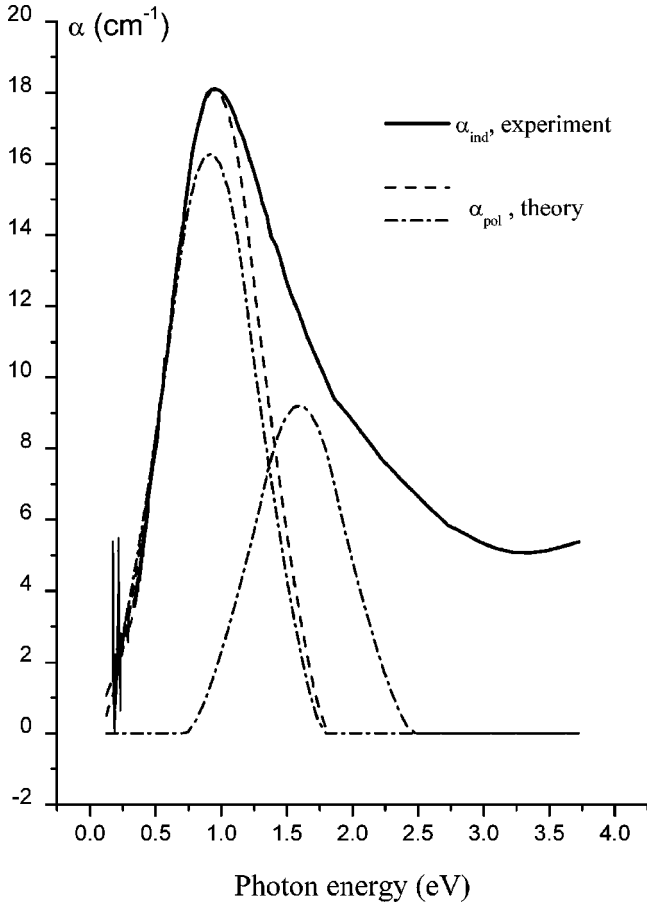


FIG. 6. Solid curve: dispersion of  $\alpha_{\text{ind}}$ , the part of the absorption coefficient induced by chemical reduction in sample 6.1 ( $C_{\text{Mg}} = 7.1$  mol %). Dashed curve: theory approximation by a single polaron resonance. Dash-dotted curves: contributions of two polaron resonances.

To obtain  $\alpha_{\text{ind}}(\omega)$ , we subtracted the intrinsic absorption of unreduced unirradiated crystals from the absorption of reduced or irradiated samples. The result for the reduced crystal of  $C_{\text{Mg}} = 7.1$  mol % (sample No. 6.1) is shown in Fig. 6 by a solid curve (as a function of the photon energy  $\hbar\omega$ ).

The broad band centered near 0.9–1 eV (1.1–1.3  $\mu\text{m}$ ), observed in the doped  $\text{LiNbO}_3$  crystals only, is attributed to small polaron absorption via polaron hopping at  $\text{Nb}_{\text{Nb}}$  sites.<sup>4,26,29</sup> Faust, Müller, and Shirmer<sup>26</sup> proposed that the hopping has an intraband character. (This means that both the start and finish of each polaron hop belong to the ground polaron band).<sup>36–39</sup> To obtain the polaron binding energy from absorption spectra, they applied the theory of intraband hopping, developed by Reik and co-workers.<sup>36,37</sup> Reik and co-workers considered the photon-assisted hopping of small polarons between next-neighbor sites.

We tried to interpret the observed  $\alpha_{\text{ind}}(\omega)$  dispersion on the basis of more general treatment, proposed by Firsov.<sup>38</sup> Firsov expanded the theory of small polaron absorption in cases when the conduction band  $\Delta\varepsilon$  is rather wide and the hopping to second and higher neighbors can also occur. It was shown that hopping at more distant sites is possible when condition  $\eta \equiv J^2/kTE_a \ll 1$  is not valid. Here  $J$  is an

electronic transfer integral between next-neighbor sites, and is proportional to  $\Delta\varepsilon$ ;  $kT$  is the temperature factor;  $E_a$  is an activation energy for the polaron hopping. The conduction band width in  $\text{LiNbO}_3$  crystals is near  $\Delta\varepsilon \sim 2.2$  eV.<sup>40</sup> Polaron hopping can occur at quite large distances, the theory parameter  $\eta$  may be rather large:  $\eta \gg 1$ .

To fit the absorption curve in Fig. 6, we used the expression

$$\text{Re } \sigma(\omega) = n_p e u_0 \frac{\omega_1}{2\omega_2} \int_0^\pi \frac{dk_y}{\pi} \int_0^\pi \frac{dk_z}{\pi} \times \left[ 1 - \left( \frac{\omega - \omega_2}{\omega_1} + \cos k_y + \cos k_z \right)^2 \right]^{1/2} \quad (2)$$

obtained by Firsov<sup>38</sup> for the real part of the electrical conductivity  $\sigma(\omega)$  in cubic crystals. Here  $\hbar\omega_1 \equiv 2J$  is responsible for the linewidth of the spectral maxima, and  $\hbar\omega_2 \equiv 2E_p$  is the energy position of the peak of  $\text{Re } \sigma(\omega)$ .  $E_p$  determines the polaron binding energy—the energy shift between the narrow ground polaron band and the wide electron conductivity band,  $E_a \approx E_p/2$ ;  $n_p$  is a polaron concentration,  $e$  is an electron charge, and the coefficient  $u_0 = ea^2/\hbar$  is of the same dimension as a charge mobility. The real part of an electrical conductivity is directly connected with the polaron contribution to an absorption coefficient:

$$\alpha_{\text{pol}}(\omega) = \frac{4\pi}{nc} \text{Re } \sigma(\omega). \quad (3)$$

Here  $n$  is a crystal refractive index. Neglecting anisotropy effects, we used Eqs. (2) and (3) to fit the experimental absorption curve for the reduced sample 6.1 (of  $C_{\text{Mg}} = 7.1$  mol %). The value of polaron shift was taken according to position of absorption maximum:  $E_p \approx 0.94/2 = 0.47$  eV. This value is close to results obtained in Ref. 26 for Mg- and Zn-doped crystals. The single matching parameter  $\omega_1 \equiv 2J/\hbar$  was selected for the best fitness of the low-energy slope of the experimental curve. It was enough to achieve a good coincidence between the observed data and the theory predictions over the whole low-energy slope. It is shown in Fig. 6, where the calculated dependence of  $\alpha_{\text{pol}}$  on the photon energy is presented by a dashed curve. As a result of fitting, we obtained the value of an electronic transfer integral:  $J = 0.145$  eV. It confirms the assumption that polaron parameter  $\eta$  is rather large in case of  $\text{LiNbO}_3$ :  $\eta \approx 3.5$ . Thus the polaron hopping occurs in  $\text{LiNbO}_3$  not only at next-neighbor sites, the charge transfer at larger distances is rather probable also.

At the same time, the account of a single polaron band is insufficient to describe the whole induced absorption in the high-energy part of the spectrum. In pure  $\text{LiNbO}_3$ , wide bands were observed at larger photon energies, centered near 2.5 and 1.6 eV. The first group was attributed to bipolaron transitions and electronic transitions from  $\text{Fe}^{3+}$  levels, the second band was considered as intraband absorption by small polarons trapped at  $\text{Nb}_{\text{Li}}$  antisites.<sup>22–29</sup> Although no isolated peaks can be selected in the residual part of an experimental absorption, we made an attempt to account for

possible absorption due to polarons trapped at  $\text{Nb}_{\text{Li}}$ , centered at 1.6 eV. It is known that, in undoped crystals of  $C_{\text{Mg}} \geq C_{\text{thr}}$ , all  $\text{Nb}_{\text{Li}}$  antisites are replaced. But the reduction procedure can create such defects.<sup>22,24</sup> Among the known absorption bands in  $\text{LiNbO}_3$ , there are no other peaks suitable to fit the experimental data in the region between the absorption maximum at 0.94 and 2 eV. Thus we assumed the sum of two contributions of the type of Eq. (3), centered at  $\omega_2^{(1)} \equiv 2E_p^{(\text{Nb}_{\text{Nb}})}/\hbar$  and at  $\omega_2^{(2)} \equiv 2E_p^{(\text{Nb}_{\text{Li}})}/\hbar$ , where  $E_p^{(\text{Nb}_{\text{Li}})} = 0.8 \text{ eV}$ —the energy shift for polarons trapped at  $\text{Nb}_{\text{Li}}$ ,  $E_p^{(\text{Nb}_{\text{Nb}})} = 0.45 \text{ eV}$ —the energy shift for polarons self-trapped at  $\text{Nb}_{\text{Nb}}$  (here we had to decrease  $E_p^{(\text{Nb}_{\text{Nb}})}$  slightly for the best two-maximum fitting). The value of  $\omega_1 \equiv 2J/\hbar$  was taken the same for the both contributions with  $J = 0.145 \text{ eV}$ , obtained in the previous fitting. In this case the single matching parameter was the relation  $n_p^{\text{Nb}_{\text{Li}}}/n_p^{\text{Nb}_{\text{Nb}}}$  between the polaron concentrations  $n_p$  at  $\text{Nb}_{\text{Li}}$  and  $\text{Nb}_{\text{Nb}}$ . It was selected for the best fitting of the experimental absorption in the region of 0.15–1.5 eV (0.8–8  $\mu\text{m}$ ). We did not state a problem to fit the higher-energy parts of the experimental curve, since had not enough information on possible resonances in this part of spectra. The results for two-maximum fitting are presented by two dotted curves in Fig. 6. Their sum describes the experimental curve in the region up to 1.5 eV (0.8  $\mu\text{m}$ ), reserving space for higher-energy resonances at shorter wavelengths. The most surprising result is that the best value for  $n_p^{\text{Nb}_{\text{Li}}}/n_p^{\text{Nb}_{\text{Nb}}}$  is 1 (within an accuracy of  $\pm 0.05$ ). This means that the number of electrons self-trapped at  $\text{Nb}_{\text{Nb}}$  is equal to the number of electrons trapped at  $\text{Nb}_{\text{Li}}$ . The last value cannot exceed the concentration of  $\text{Nb}_{\text{Li}}$  defect ions. In crystal 6, the most of  $\text{Nb}_{\text{Li}}$  defect ions are replaced by  $\text{Mg}_{\text{Li}}$ . After reduction,  $\text{Nb}_{\text{Li}}$  defect ions appear in the crystal 6.1, but their concentration is smaller than in crystal 2.1, where such defects also exist before reduction. Thus the maximal polaron concentration, which can be obtained after reduction, is limited by a number of  $\text{Nb}_{\text{Li}}$  defect ions. Partly, this explains the low values of polaron absorption induced by reduction in crystal 6.1. The induced absorption in this crystal was sufficiently less than that in crystal 2.1, though the reduction temperature was higher.

This result allows one to make a presumption that the concentration of polarons, obtained under a chemical reduction, cannot be sufficiently more than the concentration of  $\text{Nb}_{\text{Li}}$  antisites in a crystal. If this condition is valid, in Mg-doped crystals, when a density of such defects is decreased by doping, all  $\text{Nb}_{\text{Li}}$  antisites can be supplied by the trapped electrons. This can inhibit polaron hopping from one  $\text{Nb}_{\text{Li}}$  antisites to another  $\text{Nb}_{\text{Li}}$  antisite under light absorption. In this case hopping to  $\text{Nb}_{\text{Nb}}$  occur, populating the polaronic levels at  $E_p^{(\text{Nb}_{\text{Nb}})}$ . The energy distance  $\Delta E_p$  between polaron levels  $E_p^{(\text{Nb}_{\text{Li}})} \approx 0.8 \text{ eV}$  and  $E_p^{(\text{Nb}_{\text{Nb}})} \approx 0.47 \text{ eV}$  is near  $\Delta E_p \approx 0.33 \text{ eV}$ . This value is close to position of the maximum, obtained in reduced crystal 2.1 and in crystal 6 after exposure to laser radiation. Thus the origin of this peak can be connected with the direct transitions between two polaron levels—at  $E_p^{(\text{Nb}_{\text{Nb}})}$  and at  $E_p^{(\text{Nb}_{\text{Li}})}$ . This peak can appear in

absorption spectra when a number of down-transitions is less than a number of up-transitions. The peak is not seen in absorption spectra of reduced crystal 6.1 due to equal populations of the two polaron levels. But it is observed in absorption spectra of reduced crystal 2.1 and unreduced crystal 6 after exposure to laser radiation. This peak becomes apparent in refractive index dispersion of all unreduced crystals (in the region 3–4  $\mu\text{m}$  in Fig. 2). In all these samples polaron concentration seems to be less than the concentration of  $\text{Nb}_{\text{Li}}$  antisites. Nevertheless, the real distribution of polaron populations and the real character of transitions under photon absorption can be much more complicated, and requires a further investigation.

The residual part of absorption  $\alpha_0(\omega)$  was nearly the same in all bulk samples. The dispersion curves for a film and other crystals are shown in Fig. 7 as a function of the photon wave number  $\nu \equiv \omega/2\pi c$ . The crystal of a threshold Mg-concentration was characterized by a slightly larger  $\alpha(\nu)$ , but the discrepancy was no more than  $0.2 \text{ cm}^{-1}$  and did not change the whole character of  $\alpha(\nu)$  dispersion in all bulk samples. Conversely, absorption of a thin 8- $\mu\text{m}$  film was sufficiently larger.

It is reasonable to suppose that the main contribution to the intrinsic absorption is connected with the presence of optical phonon resonances, which are not far from the considered IR region. The nearest longitudinal optical phonon resonance is at  $880 \text{ cm}^{-1}$ . There are no general expressions, specifying the lattice contribution to absorption at such spectral distances precisely. To estimate the lattice contribution to absorption  $\alpha_{\text{latt}}(\nu)$  we used the oscillator formula<sup>41</sup>

$$\epsilon(\nu) = \epsilon_\infty + \sum_j \frac{S_j \nu_j^2}{\nu_j^2 - i\nu\gamma_j - \nu^2}. \quad (4)$$

$\nu_j$  and  $\gamma_j$  are the transverse phonon frequencies and damping constants (in  $\text{cm}^{-1}$ ),  $S_j$  are the phonon oscillator strengths, and  $\alpha_{\text{latt}}(\nu) = 2\pi\nu\epsilon''/\sqrt{(\epsilon' + |\epsilon|)/2}$ . We estimated  $\alpha_{\text{latt}}(\nu)$  as a mean between ordinary and extraordinary absorption values, the last were calculated through  $\epsilon''_{\perp}$  and  $\epsilon''_{\parallel}$  according to Eq. (4). Parameters of eight phonon modes with  $E$  perpendicular to the  $c$  axis and of five phonon modes with  $E$  parallel to the  $c$  axis, obtained by Barker and Loudon,<sup>42</sup> were taken to estimate  $\epsilon''_{\perp}$  and  $\epsilon''_{\parallel}$ . The phonon parameters used were determined over Raman and IR reflectivity spectra measurements for pure stoichiometric  $\text{LiNbO}_3$ . Phonon parameters variations, caused by Li deficit and Mg doping in our crystals, were later studied by Raman spectroscopy.<sup>43</sup> It was shown that only the lowest-frequency part of the phonon spectrum changes. The contribution of such changes to the lattice absorption in the considered spectral range is negligible.

As seen in Fig. 7, values of  $\alpha_{\text{latt}}$  are much larger than the measured absorption for bulk crystals. This may be due to a large spectral distance between the considered region and phonon frequencies. The nearest transverse phonon resonances are at  $670$  and  $692 \text{ cm}^{-1}$ ; the resonances, which make the largest contribution to a dielectric constant, are at  $586$  and  $628 \text{ cm}^{-1}$ . Barker and Loudon also mentioned<sup>42</sup> that the oscillator formula did not fit the absorption losses far from

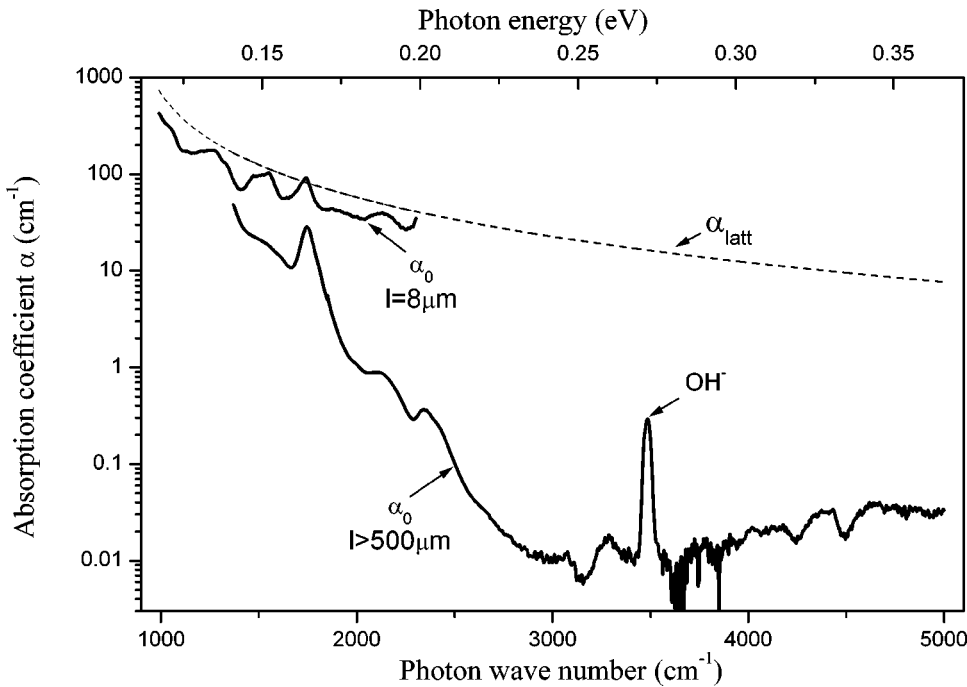


FIG. 7. Dispersion of the basic absorption coefficient  $\alpha_0(\nu)$ , measured for bulk unreduced samples of thickness  $l \geq 500 \mu\text{m}$  and for a thin crystal film  $l = 8 \mu\text{m}$  (solid curves). Dashed curve: calculation of the lattice contribution to absorption coefficient  $\alpha_{\text{latt}}(\nu)$  according to oscillator formula (4).

transverse phonon frequencies—at longitudinal phonon frequencies in their measurements. However it is interesting to note that the results on absorption in a thin film are not far from the oscillator formula predictions.

Besides a large difference in values, there is a discrepancy in the spectral behavior of  $\alpha_0(\nu)$  and of  $\alpha_{\text{latt}}(\nu)$ , calculated on the basis of the oscillator formula.  $\alpha_{\text{latt}}(\nu)$  monotonically decreases when the spectral distance from phonon resonances increases.  $\alpha_0(\nu)$  also decreases, but in addition, it is modulated with a rather stable period of order of  $\sim 200 \text{ cm}^{-1}$ . The period is comparable to the lowest frequencies of longitudinal optical phonons in  $\text{LiNbO}_3$ . At a room temperature these phonons are excited, since their energies are of

order of  $kT$ . The modulation looks similar to fine structure of absorption spectra of  $p$ -type  $\text{LaCoO}_2$ , observed by Mühlstroh and Reik.<sup>37</sup> It is seen in Fig. 7, that the modulation at  $\sim 200 \text{ cm}^{-1}$  is much more pronounced in case of the thin film. It seems that the discrepancy in modulation amplitudes is too large to explain this only by an imperfection of the used procedure of reflection losses extraction. The positions of seven maxima coincide in all crystals—bulk and extremely thin. It is shown in Fig. 8, where maxima in bulk and thin samples are presented in a logarithmic scale.

To present maxima, we subtracted a background in  $\alpha_0(\nu)$  dependences. An increase of the background  $\alpha_{\text{back}}(\nu)$  under frequency decreasing is easily approximated by an exponen-

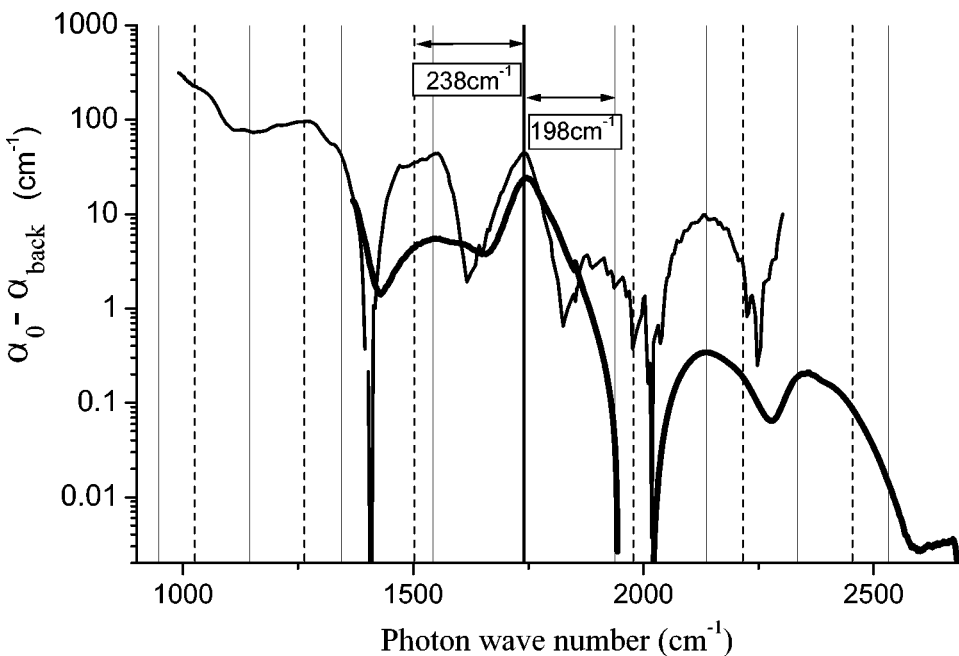


FIG. 8. Maxima at  $\alpha_0(\nu)$  dispersions after subtraction of exponential background contributions. Heavy line: for bulk samples; narrow line: for a thin film  $l = 8 \mu\text{m}$ . Vertical grid lines indicate the main peak at  $1740 \text{ cm}^{-1}$  and wave numbers, which are remote from this peak at distances, divisible by 198 and  $238 \text{ cm}^{-1}$  (see the text).

tial dependence. The exponential dependencies are the same for all bulk samples, differing from the exponential background of the thin-film absorption. Vertical grid lines indicate the main peak at  $1740\text{ cm}^{-1}$  and frequencies, which are remote from this peak at distances, divisible by 198 and  $238\text{ cm}^{-1}$ : at  $1740 \pm p \times 198\text{ cm}^{-1}$  and  $1740 \pm p \times 238\text{ cm}^{-1}$ . Integer  $p$  is equal to 1, 2, 3, and  $198\text{ cm}^{-1}$  and  $238\text{ cm}^{-1}$  are the frequencies of the lowest optical longitudinal phonons.<sup>42</sup> The positions of the observed maxima coincide with these frequencies with a fairly good accuracy. However, this is probably only one of possible assignments of the observed maxima.

Up to now we cannot explain unambiguously the modulation appearance and its sensitivity to the dimension lowering. It is clear only that peaks do not appear due to direct absorption at two- or three-phonon combination bands, since they are observed in a large range of spectra (see Fig. 5) with a rather high periodicity. It seems reasonable to regard the appearance of regular phonon iteration peaks to be a result of an electron-phonon interaction, and to make a search for an additional contribution of structure defects to absorption at low frequencies. Since the modulation does not change after reduction or irradiation, this contribution should be independent of the polaron concentration.

## V. SUMMARY

We have measured refractive indices (see Table II and Figs. 1 and 2) and absorption coefficients (Figs. 3–5) for Mg:LiNbO<sub>3</sub> single crystals of different Mg contents in the visible and IR ranges up to a phonon absorption edge. It was shown that, after a chemical reduction of Mg:LiNbO<sub>3</sub> crystals of high Mg concentration, a wide absorption band emerges in the transparency region of pure LiNbO<sub>3</sub> crystals, being centered at  $1.3\ \mu\text{m}$ . The main contribution to absorption, induced in Mg:LiNbO<sub>3</sub> at  $1.3\text{--}8\ \mu\text{m}$  by a chemical reduction, is due to hopping of small polarons. Our data do not contradict to the previously made assumption that the trapping occurs at regular Nb<sub>Nb</sub> sites in a crystal lattice. According to our estimations, the polaron shift  $E_p \approx 0.45\text{--}0.47\text{ eV}$ , the value of an electronic transfer integral  $J = 0.145\text{ eV}$ . Hopping at second and higher-neighbor Nb<sub>Nb</sub> sites take place. In the region of  $0.4\text{--}1.3\ \mu\text{m}$ , additional mechanisms of absorption should be considered to explain the induced absorption. In particular, the contribution due to hopping of small polarons, which are trapped at Nb<sub>Li</sub> antisites, is rather large. The theory approximation of the induced absorption by two polaron contributions, with maxima

at 0.9 and 1.6 eV, shows that polaron concentrations at Nb<sub>Li</sub> antisites and at Nb<sub>Nb</sub> sites coincide in a reduced crystal of Mg concentration above the photorefractive threshold.

An additional absorption band was registered near  $3.2\ \mu\text{m}$  (0.38 eV) in a number of Mg-doped crystals. It can become stronger after exposition to power laser radiation or chemical reduction of crystals with the proper level of Mg concentration. We assign this band to optical transitions between Nb<sub>Li</sub> and Nb<sub>Nb</sub> polaron levels.

Also, our spectral dependencies of deviation between ordinary refractive indices of the unreduced Mg-doped crystals and of pure LiNbO<sub>3</sub> reveal weak resonance bands in two spectral ranges: centered near  $1.3$  and  $3.2\ \mu\text{m}$ . The resonances are too intense to fit the spectral dependences of usual Mg:LiNbO<sub>3</sub> by any Sellmeier-type expressions within the pertinent absolute accuracy.

The residual parts of absorption, obtained after subtraction of all chemically or light induced effects, almost coincide in all Mg-doped crystals in the studied spectral range of  $1200\text{--}5000\text{ cm}^{-1}$ . The weak absorption dependencies on the Mg-concentration have the same character as the ordinary refractive index dependencies at constant wavelength in the range  $4\text{--}5\ \mu\text{m}$ . All Mg-concentration dependencies for usual unreduced crystals in this IR range indicate the four-step character of structural changes under subsequent Mg doping.

The intrinsic (uninduced) part of absorption near the phonon absorption edge is characterized by a number of peculiarities. First the values of the intrinsic absorption are sufficiently less than those predicted by phonon oscillator formula. Second, its spectral dependencies are modulated at a rather stable period, being of order of the frequencies of the lowest-energy longitudinal optical phonons excited at room temperature. The amplitude of modulation is different in different spectral regions and is much larger in a thin crystal film of  $8\text{-}\mu\text{m}$  thickness. We assume, that the observed modulation is a result of an electron-phonon interaction, but further investigation is required to explain this completely.

## ACKNOWLEDGMENTS

The authors are grateful to I. I. Naumova, who grew and kindly supplied the crystals, to A. A. Mikhailovsky and V. F. Morosova for the help, and to S. V. Lavrishchev and V. N. Talanova for an independent x-ray analysis of the Mg impurity in the samples. This work was supported by the Russian Foundation for Basic Research (Grant Nos. 99-02-16418, and 00-15-96541) and the Russian Federal Program "Integration: Fundamental optics and spectroscopy."

<sup>1</sup>R. L. Byer, *J. Nonlinear Opt. Phys. Mater.* **6**, 549 (1997).

<sup>2</sup>A. M. Glass, *Science* **222**, 657 (1984).

<sup>3</sup>K. Buse, *Appl. Phys. B: Lasers Opt.* **64**, 391 (1997).

<sup>4</sup>T. Volk and M. Wöhlecke, *Ferroelect. Rev.* **1**, 195 (1998).

<sup>5</sup>M. Wöhlecke, G. Corradi, and K. Betzler, *Appl. Phys. B: Lasers Opt.* **63**, 323 (1996).

<sup>6</sup>Y. Furukawa, K. Kitamura, S. Takekawa, K. Niwa, Y. Yajima, N.

Iyi, I. Mnushkina, P. Guggenheim, and J. Martin, *J. Cryst. Growth, Phys. Lett.* **211**, 230 (2000).

<sup>7</sup>M. V. Hobden and J. Warner, *Phys. Lett.* **22**, 243 (1966).

<sup>8</sup>J. G. Bergman, A. Ashkin, A. A. Ballman, J. M. Dziedzic, H. J. Levinstein, and R. G. Smith, *Appl. Phys. Lett.* **12**, 92 (1968).

<sup>9</sup>D. F. Nelson and R. M. Mikulyak, *J. Appl. Phys.* **45**, 3688 (1974).

<sup>10</sup>D. S. Smith, H. D. Riccius, and R. P. Edwin, *Opt. Commun.* **17**,

- 332 (1976).
- <sup>11</sup>G. M. Georgiev, G. Kh. Kitaeva, A. G. Mikhailovsky, A. N. Penin, N. M. Rubinina, *Fiz. Tverd. Tela (Leningrad)* **16**, 3524 (1974) [*Sov. Phys. Solid State* **16**, 2293 (1975)].
- <sup>12</sup>A. L. Aleksandrovskii, G. I. Ershova, G. Kh. Kitaeva, S. P. Kulik, I. I. Naumova, and V. V. Tarasenko, *Kvant. Electron. (Moscow)* **18**, 254 (1994) [*Quantum Electron.* **21**, 225 (1991)].
- <sup>13</sup>H. Y. Shen, H. Xu, Z. D. Zeng, W. X. Lin, R. F. Wu, and G. F. Xu, *Appl. Opt.* **31**, 6695 (1992).
- <sup>14</sup>U. Schlarb and K. Betzler, *Phys. Rev. B* **48**, 15 613 (1993).
- <sup>15</sup>U. Schlarb and K. Betzler, *Phys. Rev. B* **50**, 751 (1994).
- <sup>16</sup>D. E. Zelmon, D. L. Small, and D. Jundt, *J. Opt. Soc. Am. B* **14**, 3319 (1997).
- <sup>17</sup>G. Kh. Kitaeva, I. I. Naumova, A. A. Mikhailovsky, P. S. Losevsky, and A. N. Penin, *Appl. Phys. B: Lasers Opt.* **66**, 201 (1998).
- <sup>18</sup>G. K. Kitaeva, K. A. Kuznetsov, I. I. Naumova, and A. N. Penin, *Kvant. Electron. (Moscow)* **30**, 726 (2000) [*Quantum Electron.* **30**, 726 (2000)].
- <sup>19</sup>J. T. Devreese, *Encyclopedia Appl. Phys.* **14**, 383 (1996).
- <sup>20</sup>T. Holstein, *Ann. Phys. (N.Y.)* **8**, 325 (1959).
- <sup>21</sup>O. F. Schirmer and D. von der Linde, *Appl. Phys. Lett.* **33**, 35 (1978).
- <sup>22</sup>O. F. Schirmer, O. Thiemann, and M. Wöhlecke, *J. Phys. Chem. Solids* **52**, 185 (1991).
- <sup>23</sup>F. Jermann, M. Simon, R. Böwer, E. Krätzig, and O. F. Schirmer, *Ferroelectrics* **165**, 319 (1995).
- <sup>24</sup>H. Donnerberg, S. M. Tomlinson, C. R. A. Catlow, and O. F. Schirmer, *Phys. Rev. B* **40**, 11 909 (1989).
- <sup>25</sup>A. Dhar and A. Mansingh, *J. Appl. Phys.* **68**, 5804 (1990).
- <sup>26</sup>B. Faust, H. Müller, and O. F. Schirmer, *Ferroelectrics* **153**, 297 (1994).
- <sup>27</sup>I. Sh. Akhmadullin, V. A. Golenishev-Kutuzov, and S. A. Migachev, *Fiz. Tverd. Tela (St. Petersburg)* **40**, 1109 (1998) [*Phys. Solid State* **40**, 1012 (1998)].
- <sup>28</sup>I. Sh. Akhmadullin, V. A. Golenishev-Kutuzov, S. A. Migachev, and S. P. Mironov, *Fiz. Tverd. Tela (St. Petersburg)* **40**, 1307 (1998) [*Phys. Solid State* **40**, 1190 (1998)].
- <sup>29</sup>T. Volk, N. Rubinina, and M. Wöhlecke, *J. Opt. Soc. Am. B* **11**, 1681 (1994).
- <sup>30</sup>D. Berben, K. Buse, S. Wevering, P. Herth, M. Imlau, and Th. Woike, *J. Appl. Phys.* **87**, 1034 (2000).
- <sup>31</sup>I. I. Naumova, *Crystallogr. Rep.* **39**, 1029 (1994).
- <sup>32</sup>H. Donnerberg, S. M. Tomlinson, C. R. A. Catlow, and O. F. Schirmer, *Phys. Rev. B* **44**, 4877 (1991).
- <sup>33</sup>D. A. Bryan, R. Gerson, and H. E. Tomaschke, *Appl. Phys. Lett.* **44**, 847 (1984).
- <sup>34</sup>K. L. Sweeney, L. E. Halliburton, D. A. Bryan, R. R. Rice, R. Gerson, and H. E. Tomaschke, *J. Appl. Phys.* **57**, 1036 (1985).
- <sup>35</sup>D. N. Klyshko, *Photons and Nonlinear Optics* (Gordon & Breach, New York, 1988).
- <sup>36</sup>H. G. Reik, *Z. Phys.* **203**, 346 (1967).
- <sup>37</sup>R. Mühlstroh and H. G. Reik, *Phys. Rev.* **162**, 703 (1967).
- <sup>38</sup>Yu. A. Firsov, *Fiz. Tverd. Tela (Leningrad)* **10**, 1950 (1968).
- <sup>39</sup>D. M. Eagles, *Phys. Rev.* **130**, 1381 (1963).
- <sup>40</sup>I. Inbar and R. E. Cohen, *Phys. Rev. B* **53**, 1193 (1996).
- <sup>41</sup>A. S. Barker, *Phys. Rev.* **145**, 391 (1966).
- <sup>42</sup>A. S. Barker and R. Loudon, *Phys. Rev.* **158**, 433 (1967).
- <sup>43</sup>L. J. Hu, Y. H. Chang, C. S. Chang, S. J. Yang, M. L. Hu, and W. S. Tse, *Mod. Phys. Lett. B* **5**, 789 (1991).